AD-A045 775 ROME AIR DEVELOPMENT CENTER GRIFFISS AFB N Y F/G 9/5
A THEORETICAL INVESTIGATION OF THE RECTANGULAR MICROSTRIP ANTEN--ETC(U)
JUN 77 A G DERNERYD

UNCLASSIFIED RADC-TR-77-206 NL

1 OF 1
ADA
045775

END
DATE
FILMED
11-77
DDC

RADC-TR-77-206
IN-HOUSE REPORT
JUNE 1977

12
B.S.

A Theoretical Investigation of the Rectangular Microstrip Antenna Element

ANDERS G. DERNERYD

ROME AIR DEVELOPMENT CENTER
AIR FORCE SYSTEMS COMMAND
GRIFFISS AIR FORCE BASE, NEW YORK 13441

This report has been reviewed by the RADC Information Office (OI) and is releasable to the National Technical Service (NTIS). At NTIS it will be releasable to the general public, including foreign nations.

This technical report has been reviewed and approved for publication.

APPROVED:

JOHN K. SCHINDLER
Acting Chief, Antenna & Radar Techniques Branch

APPROVED:

ALLAN C. SCHELL
Acting Chief
Electromagnetic Sciences Division

FOR THE COMMANDER:

Plans Office

Unclassified

SECURITY CLASSIFICATION OF THIS PAGE (When Data Entered)

REPORT DOCUMENTATION PAGE		READ INSTRUCTIONS BEFORE COMPLETING FORM
1. REPORT NUMBER: RADC-TR-77-206	2. GOVT ACCESSION NO.	3. RECIPIENT'S CATALOG NUMBER
4. TITLE (and Subtitle): A THEORETICAL INVESTIGATION OF THE RECTANGULAR MICROSTRIP ANTENNA ELEMENT.		5. TYPE OF REPORT & PERIOD COVERED: In-House
		6. PERFORMING ORG. REPORT NUMBER
7. AUTHOR(s): Anders G. Derneryd		8. CONTRACT OR GRANT NUMBER(s): Technical rept.
9. PERFORMING ORGANIZATION NAME AND ADDRESS: Deputy for Electronic Technology (RADC/ETE) Hanscom AFB Massachusetts 01731		10. PROGRAM ELEMENT, PROJECT, TASK AREA & WORK UNIT NUMBERS: 62702F 4600
11. CONTROLLING OFFICE NAME AND ADDRESS: Deputy for Electronic Technology (RADC/ETE) Hanscom AFB Massachusetts 01731		12. REPORT DATE: June 1977
		13. NUMBER OF PAGES: 23
14. MONITORING AGENCY NAME & ADDRESS (if different from Controlling Office)		15. SECURITY CLASS. (of this report): Unclassified
		15a. DECLASSIFICATION/DOWNGRADING SCHEDULE

16. DISTRIBUTION STATEMENT (of this Report)

Approved for public release; distribution unlimited.

17. DISTRIBUTION STATEMENT (of the abstract entered in Block 20, if different from Report)

18. SUPPLEMENTARY NOTES

19. KEY WORDS (Continue on reverse side if necessary and identify by block number)

Theoretical investigation
Rectangular microstrip antenna
Network model
Mutual conductance

20. ABSTRACT (Continue on reverse side if necessary and identify by block number)

A theoretical treatment of the rectangular microstrip radiating element has been performed. The element has been modeled as a line resonator with radiation taking place at the open-circuited ends. With this simplified model, the input impedance and the far-fields have been calculated for different resonance modes. The interaction between the radiating ends will effect the input impedance and this has been considered by defining a mutual conductance. Also, a mutual conductance between microstrip elements has been expressed

NEXT Page →

DD FORM 1 JAN 73 1473 EDITION OF 1 NOV 65 IS OBSOLETE

Unclassified

SECURITY CLASSIFICATION OF THIS PAGE (When Data Entered)

309 050

4B

20. Abstract (Continued)

in far-field quantities and plotted as a function of spacing along the E- and H-planes. The directivity of an isolated element has been calculated as the directivity of one radiating end times the contribution due to the array factor.

Contents

Illustrations

A Theoretical Investigation of the Rectangular Microstrip Antenna Element

1. INTRODUCTION

The microstrip antenna consists of a radiating structure spaced a small fraction of a wavelength above a ground plane. Antennas of this type have found applications where cost, weight, and ruggedness are important factors. Most of the work reported so far has been experimental. However, the circular disc microstrip element has theoretically been treated as a cavity[1] while the rectangular patch has been modeled as a pair of slots separated by a transmission line.[2, 3] A different approach has been presented[4] where the radiating structure is modeled

(Received for publication 17 June 1977)

1. Howell, J.Q. (1975) Microstrip antennas, IEEE Trans. Antennas Propagat. AP-23:90-93.
2. Munson, R.E. (1974) Conformal microstrip antennas and microstrip phased arrays, IEEE Trans. Antennas Propagat. AP-22:74-78.
3. Derneryd, A.G. (1976) Linearly polarized microstrip antennas, IEEE Trans. Antennas Propagat. AP-24:846-851.
4. Agrawal, P.K. and Bailey, M.C. (1976) An analysis technique for microstrip antennas, IEEE Society on Antennas Propagat. Int. Symp.:395-398.

as a fine grid of wire segments. Some basic design formulas for microstrip patch antennas have also been reported.[5, 6]

In this paper, the rectangular microstrip radiating element is theoretically investigated. The input impedance and the resonant length are calculated by considering the element as a line resonator with the open-circuited terminations modeled as an RC network. From a radiation point of view the element is treated as two narrow slots, one at each end of the line resonator. The interaction between the two slots is considered by defining a mutual conductance. From the far-fields, the directivity of both a slot and a patch are calculated. The mutual conductance between patches is expressed in terms of far-field components alone.

2. LINE RESONATOR

A rectangular microstrip radiating element is schematically shown in Figure 1. The element is fed with a transmission line in the plane of the patch or from the back through the ground plane to give a field distribution which is uniform along the width. This is achieved either by making the width of the element shorter than a half dielectric wavelength or by using many feed points separated by a wavelength. Therefore this structure can be treated as a transmission line which is open-circuited at both ends and supports quasi – TEM modes. The resonance frequencies must, to a first approximation, be a multiple of the half dielectric wavelength:

$$f_n = n \cdot \frac{c_o}{2 \cdot L \cdot \sqrt{\epsilon_{eff}}} \qquad (1)$$

where c_o is the velocity of light and ϵ_{eff} is the effective dielectric constant of a microstrip line of width W and length L.

At the lowest resonance frequency, the fields at the ends are reversed as illustrated in Figure 1. The horizontal components of the fringing fields at either end are in phase and give a maximum radiated field normal to the patch. The vertical components and the fringing fields along the sides don't give any contribution at broadside but will have a minor influence on the far-fields for angles off boresight.

---

5. Kaloi, C. M. (1975) Asymmetrically Fed Electric Microstrip Dipole Antenna, Report TP-75-03, Naval Missile Center, Point Magu, CA.

6. Black, L. M., and McCorkle, J. W. (1975) A Preliminary Report on the In-house Exploratory Development Program on Microstrip Patch Antennas at Naval Surface Weapons Center, Report NSWC/WOL/TR 75-200, Naval Surface Weapons Center, Silver Spring, MD.

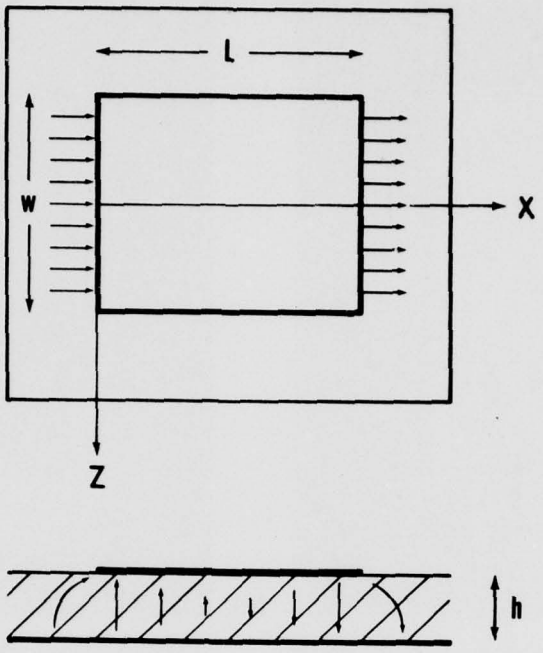

Figure 1. Rectangular Microstrip Radiating Element

The fringing fields of the resonator can be viewed by means of a liquid crystal detector.[7] By placing the detector* above the patch, the fields in the plane of the detector can be visually observed. Three different detector displays of the resonance mode structures on same microstrip element are shown in Figure 2. The radiation takes place at the ends of the line resonator and the microstrip element, therefore, essentially behaves as two slots. At the higher order resonance modes, standing wave maxima are observed along the patch separated by a half dielectric wavelength.

The fields at the ends of the line resonator can be represented by an equivalent uniform magnetic current along the Z-axis. This approximation is reasonable as long as the ground plane spacing is very small; that is, $k_o h \ll 1$ where k_o is the propagation constant. The far-fields of a uniformly illuminated narrow slot expressed in standard spherical coordinates are:

---

*The microwave liquid crystal detector was supplied by James Sethares.

7. Kernweis, N.P., and McIlvenna, J.F. Liquid crystal diagnostic techniques aid microstrip antenna design, pending publication in Microwave Journal.

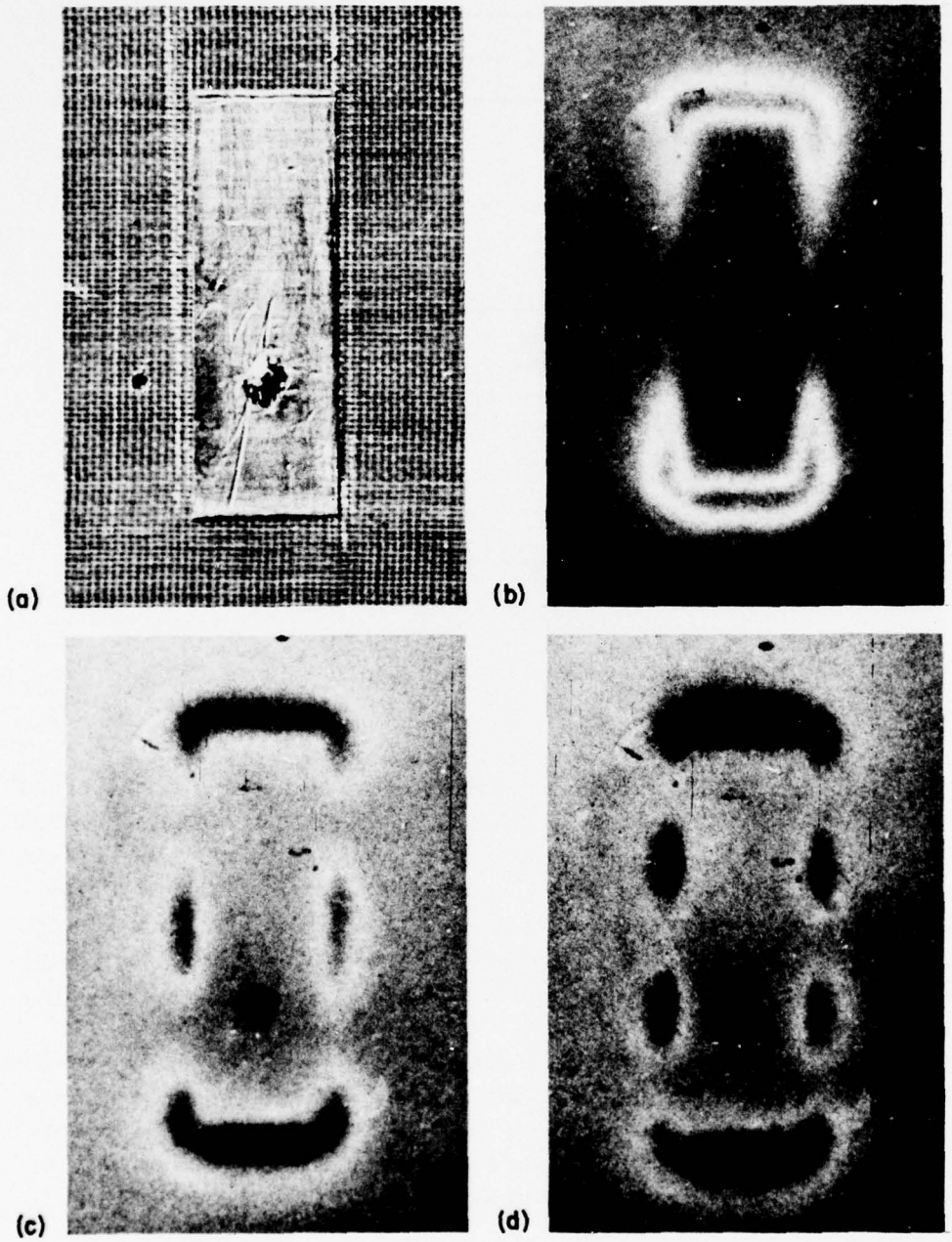

Figure 2. Liquid Crystal Displays of a Rectangular Microstrip Element Excited in Different Modes. (a) Microstrip element, (b) first mode, 3.10 GHz; (c) second mode, 6.15 GHz; (d) third mode, 9.15 GHz

$$\begin{cases} E_{\Phi} = -j \cdot \dfrac{V_o}{\pi} \cdot \dfrac{e^{-jk_o r}}{r} \cdot \dfrac{\sin\left(\dfrac{\pi w}{\lambda_o} \cdot \cos\theta\right)}{\cos\theta} \cdot \sin\theta \\ H_{\theta} = -\sqrt{\dfrac{\epsilon}{\mu}} \cdot E_{\Phi} \end{cases} \tag{2}$$

where V_o is the voltage across the slot and λ_o is the wavelength in free space. The far-fields are linearly polarized and independent of the ground plane spacing h, as long as this is a small fraction of a wavelength.

3. NETWORK MODEL

The radiation at the open-circuited ends of the line resonator can be represented by a radiation conductance. This is defined as a conductance which will dissipate the same power as that radiated by the slot:

$$G = \frac{1}{\pi} \cdot \sqrt{\frac{\epsilon}{\mu}} \int_0^{\pi} \frac{\sin^2\left(\dfrac{\pi w}{\lambda_o} \cdot \cos\theta\right)}{\cos^2\theta} \cdot \sin^3\theta \cdot d\theta \quad . \tag{3}$$

This integral has been solved numerically and a plot of the radiation conductance as a function of the width can be found in Derneryd.[3]

The effect of the fringing fields at the ends of the line resonator can be represented either as a shunt capacitance or as a lengthening of the line. In both cases, the end effect can be modeled as an equivalent susceptance. The microstrip element can, therefore, be modeled as a network with two admittances separated by a transmission line of width W and length L as shown in Figure 3.

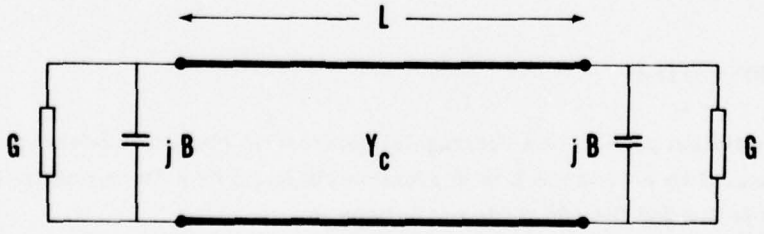

Figure 3. Network Model of the Microstrip Radiating Element

The resonant length of the element is defined as the length at which the input admittance is pure real. The input admittance is found by transforming the slot admittances to the feed point and adding them in parallel. The resonant length is given by:

$$\tan \beta L = \frac{2 \cdot B \cdot Y_c}{G^2 + B^2 - Y_c^2} \tag{4}$$

where β is the propagation constant in the dielectric. The resonant length depends on the width of the element, the ground plane spacing, and the dielectric constant but it is independent of feed point location as long as quasi - TEM modes are excited. An effective dielectric constant has to be defined taking into account the fringing fields along the sides before the propagation constant can be determined.

In most practical cases, the characteristic admittance of the transmission line, Y_c, is much greater than both the radiation conductance and the equivalent susceptance. Therefore, by solving Eq. (4) the resonant lengths can be expressed as:

$$L = n \cdot \frac{\lambda_g}{2} - 2 \cdot \Delta L \quad . \tag{5}$$

That is, the resonant length of an element is a multiple of a half dielectric wavelength corrected by a term ΔL, which represents the extension of the terminal plane from the physical open end due to the end capacitance C. The line extension is expressed as:

$$\Delta L = \frac{v \cdot C}{Y_c} \tag{6}$$

where v is the velocity in the dielectric. The resonance frequency of the microstrip element is thus decreased a small fraction if the effective length is used in the calculations.

4. RADIATION PATTERN

The radiation pattern of a rectangular microstrip element modeled as two slots separated by a distance L is approximately found by pattern multiplication. The array factor for the odd mode excitations is

$$AF_o = 2 \cdot \cos\left(\frac{\pi L}{\lambda_o} \cdot \sin\theta \cdot \cos\Phi\right) \quad . \tag{7}$$

For the even modes, the horizontal components of the fringing fields are out-of-phase and, therefore, the array factor becomes

$$AF_e = 2 \cdot \sin\left(\frac{\pi L}{\lambda_o} \cdot \sin\theta \cdot \cos\Phi\right) \quad . \tag{8}$$

The radiation pattern of a microstrip element along a vertical cut in the E-plane is determined by the array factor alone since the far-fields of a slot are constant in this plane. Along the H-plane, the array factor for odd mode excitation is constant while it is zero for the even modes. Therefore, the radiation patterns of the odd modes are completely determined by the element pattern of the slot.

Radiation patterns of a rectangular microstrip element with the dimensions 10 mm $\times$ 30.5 mm have been recorded for the first three resonance modes. The vertical cuts along the E-plane are shown in Figures 4 through 6. As comparison, the theoretical radiation patterns are also included in the figures as dotted lines. The minor fluctuations in the recorded patterns are due to the finite ground plane (0.61 m $\times$ 0.61 m). A vertical cut of the radiation pattern along the H-plane of the lowest mode is shown in Figure 7. The two slot model of the microstrip radiating element gives very good agreement between theory and practice except in the region close to endfire.

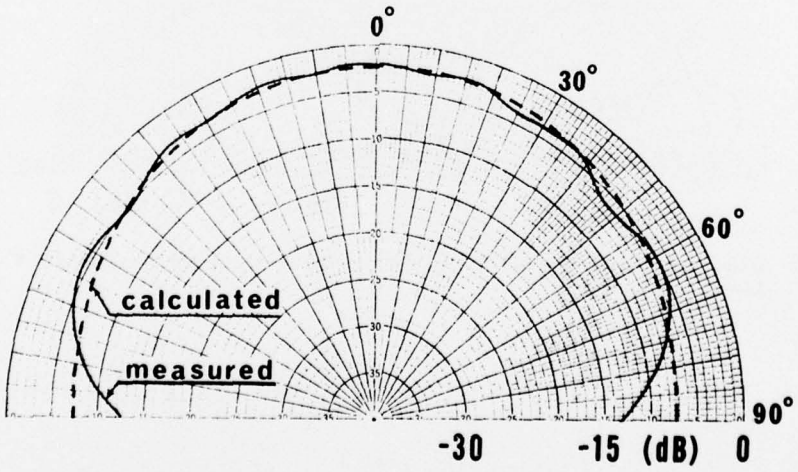

Figure 4. Radiation Pattern Along the E-plane of the First Mode, 3.10 GHz

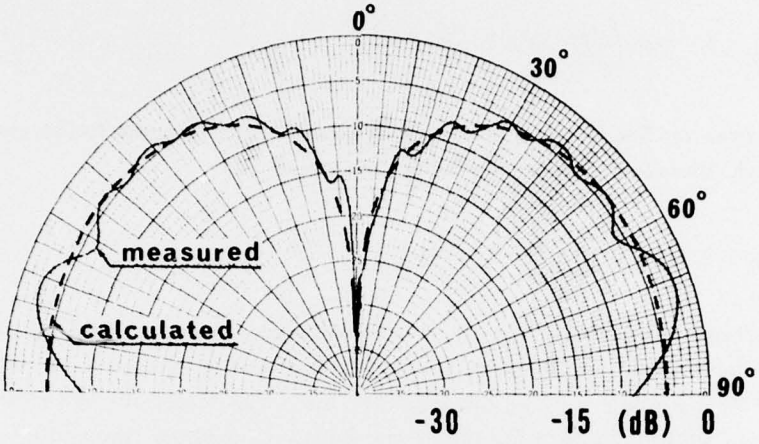

Figure 5. Radiation Pattern Along the E-plane of the Second Mode, 6.15 GHz

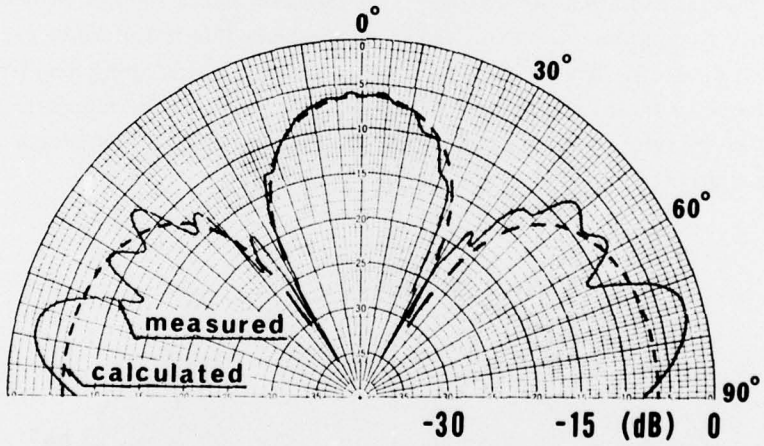

Figure 6. Radiation Pattern Along the E-plane of the Third Mode, 9.15 GHz

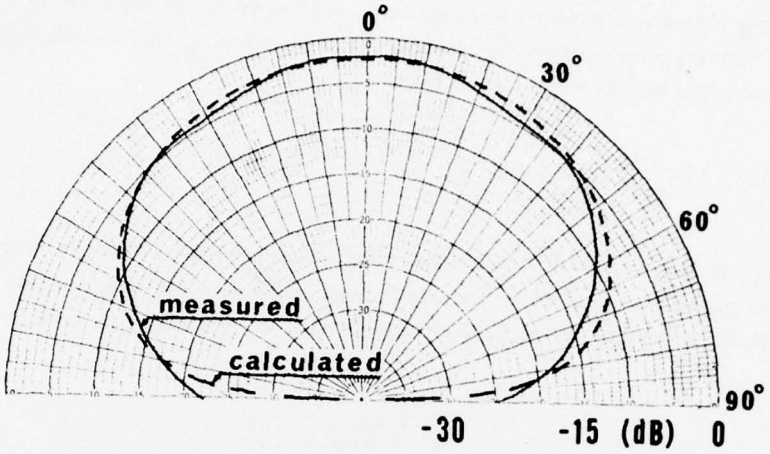

Figure 7. Radiation Pattern Along the H-plane of the First Mode, 3.10 GHz

5. INPUT IMPEDANCE

The input impedance for different feed point locations can be calculated with the network model. At resonance, the input impedance at an arbitrary feed point, a distance χ from one end of the microstrip element is pure real. By transforming the slot admittances to the common point and adding them together, the input impedance at resonance is found to be:

$$Z_{in}(\chi) = \frac{1}{2 \cdot G} \left(\cos^2 \beta\chi + \frac{G^2 + B^2}{Y_c^2} \cdot \sin^2 \beta\chi - \frac{B}{Y_c} \cdot \sin 2\beta\chi \right) \tag{9}$$

Usually $\frac{G}{Y_c} \ll 1$ and $\frac{B}{Y_c} \ll 1$ and therefore (9) simplifies to:

$$Z_{in}(\chi) = \frac{1}{2 \cdot G} \cdot \cos^2 \beta\chi \tag{10}$$

except close to the center of the element.

The mutual effect between the two slots is not included in the above formulas. The behavior of two coupled antennas can be described by network concepts. The relation between the voltages and the currents at the input terminals is then represented by an admittance matrix. The corresponding network for two identical

radiators is drawn in Figure 8. At resonance, the voltages at the ends of the microstrip element are equal in magnitude and the phase difference is a multiple of 180^{o}. Taking into account the mutual conductance G_{12}, the expression for the input impedance has to be modified to:

$$Z_{in}(\chi) = \frac{1}{2(G_{11} \pm G_{12})} \cdot \cos^2 \beta\chi \tag{11}$$

where G_{11} is the radiation conductance of an isolated slot. The plus sign corresponds to the odd modes while the minus sign refers to the even modes. The denominator is simply the radiation conductance of a patch at resonance.

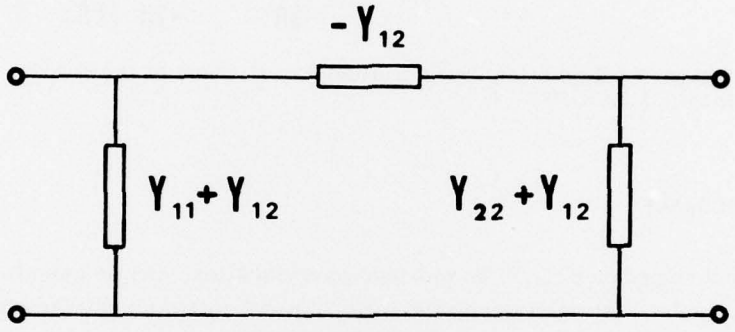

Figure 8. Network Representation of a Pair of Coupled Antennas

6. MUTUAL CONDUCTANCE

A mutual conductance between two antennas can be derived by considering the total radiated power in a manner similar to that used to define the radiation conductance for an isolated antenna. If the antennas are excited by equal voltages, the mutual conductance expressed in far-field components is:

$$G_{12} = \frac{1}{|V_o|^2} \cdot \mathrm{Re} \int \bar{E}_1 \times \bar{H}_2^{*} \, \overline{ds} \tag{12}$$

where $\overline{ds}$ is a vector normal to a sphere of large radius and the asterisk denotes the complex conjugate.

6.1 Slots

Consider two slots of length W placed in the X-Z plane and aligned in the Z-direction. The mutual conductance when radiating into half space is:

$$G_{12} = \frac{1}{\pi} \cdot \sqrt{\frac{\epsilon}{\mu}} \int_0^{\pi} \frac{\sin^2\left(\frac{\pi W}{\lambda_o} \cdot \cos\theta\right)}{\cos^2\theta} \cdot \sin^3\theta \cdot J_o\left(\frac{\chi}{\lambda_o} \cdot 2\pi \cdot \sin\theta\right) \cdot$$

$$\cdot \cos\left(\frac{Z}{\lambda_o} \cdot 2\pi \cdot \cos\theta\right) \cdot d\theta \qquad (13)$$

where J_o is the zero-order Bessel function of the first kind. At zero spacing, Eq. (13) gives the radiation conductance (3) of an isolated slot.

Values of this integral have been calculated for two special cases. The normalized mutual conductance between two narrow slots along the E-plane is shown in Figure 9 as a function of spacing. The longer the slot, the stronger is the coupling. The corresponding curves for coupling along the H-plane are plotted in Figure 10. As expected, the coupling decreases much more rapidly.

6.2 Patches

The mutual conductance between two rectangular microstrip elements is found from Eq. (2) and (12) together with (7) or (8). Along the E-plane, the mutual conductance between patches with length L and width W excited in the odd modes is:

$$G_{12} = \frac{1}{\pi} \cdot \sqrt{\frac{\epsilon}{\mu}} \int_0^{\pi} \frac{\sin^2\left(\frac{\pi W}{\lambda_o} \cdot \cos\theta\right)}{\cos^2\theta} \cdot \sin^3\theta \cdot \left\{ 2 \cdot J_o\left(\frac{\chi}{\lambda_o} \cdot 2\pi \cdot \sin\theta\right) + \right.$$

$$\left. + J_o\left(\frac{\chi + L}{\lambda_o} \cdot 2\pi \cdot \sin\theta\right) + J_o\left(\frac{\chi - L}{\lambda_o} \cdot 2\pi \cdot \sin\theta\right) \right\} d\theta \quad . \qquad (14)$$

The first term in Eq. (14) is twice the mutual conductance between two slots along the E-plane spaced by a distance χ. The second and the third term are the coupling between two slots separated by distances $\chi + L$ and $\chi - L$ along the E-plane. The approximation used to derive (14) is that the far-fields of a patch are determined by the element factor times the array factor.

The integrals in (14) have been computed numerically and the results are shown in Figure 11. The mutual coupling between two patches along the H-plane for odd modes is:

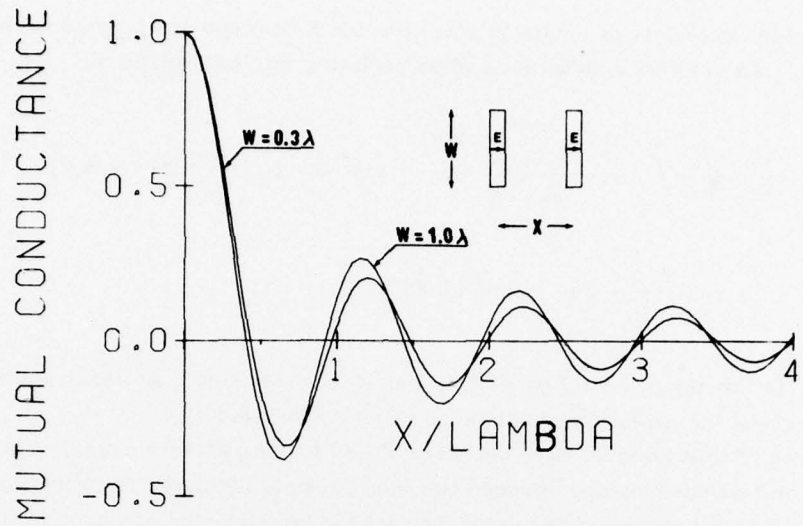

Figure 9. Normalized Mutual Conductance Between Two Narrow Slots Along the E-plane

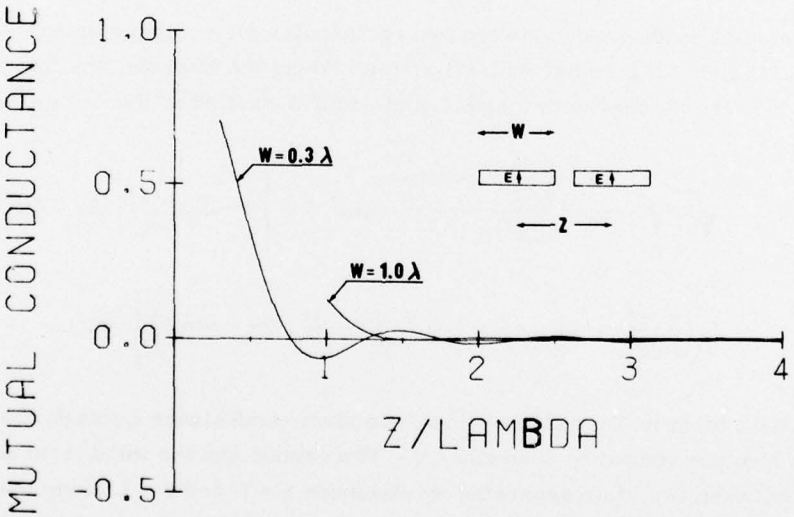

Figure 10. Normalized Mutual Conductance Between Two Narrow Slots Along the H-plane

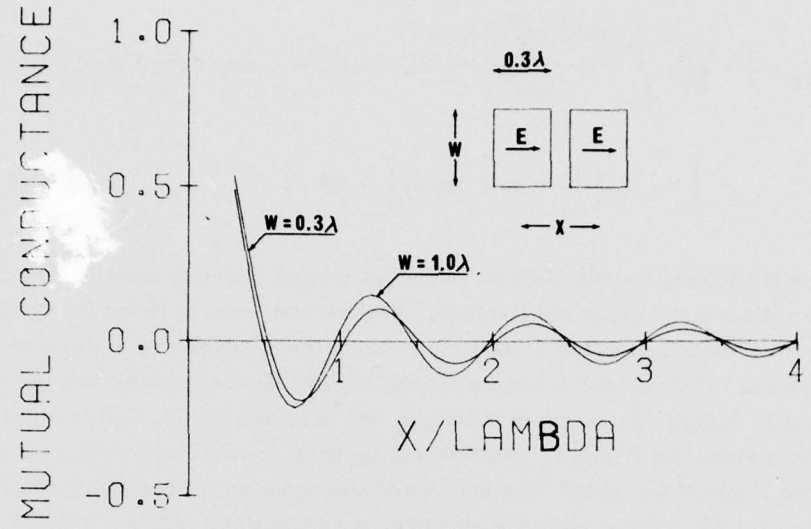

Figure 11. Normalized Mutual Conductance Between Two Rectangular Microstrip Elements Along the E-plane

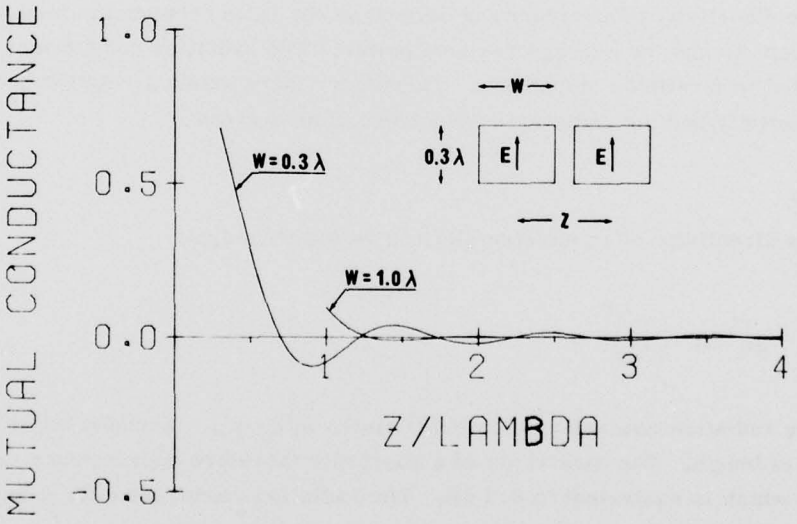

Figure 12. Normalized Mutual Conductance Between Two Rectangular Microstrip Elements Along the H-plane

$$G_{12} = \frac{2}{\pi} \cdot \sqrt{\frac{\epsilon}{\mu}} \int_0^{\pi} \frac{\sin^2\left(\frac{\pi w}{\lambda_o} \cdot \cos\theta\right)}{\cos^2\theta} \cdot \sin^3\theta \cdot \cos\left(\frac{Z}{\lambda_o} \cdot 2\pi \cdot \cos\theta\right) \cdot$$

$$\cdot \left\{1 + J_o\left(\frac{L}{\lambda_o} \cdot 2\pi \cdot \sin\theta\right)\right\} \cdot d\theta \quad . \tag{15}$$

The first term is identified as twice the mutual coupling between two slots spaced a distance Z along the H-plane. The second term is twice the coupling between two slots separated a distance L along the E-plane and a distance Z along the H-plane. The normalized mutual coupling has been computed and the result is drawn in Figure 12. As with the slots, the coupling decays faster along the H-plane than along the E-plane. An interesting point is that the coupling is stronger along the E-plane for wider elements while the opposite is true along the H-plane. Patches excited in the even mode resonances can be analyzed in a similar way.

7. DIRECTIVITY

The directivity of an antenna is defined as the ratio between the maximum power density and the average radiated power. The radiation conductance is also expressed in far-field components. Therefore, there exists a relation between the directivity and the radiation conductance of an antenna.

7.1 Slots

The directivity of an isolated slot can be expressed as:

$$D_o = \frac{1}{30 \cdot G} \left(\frac{w}{\lambda_o}\right)^2 \quad . \tag{16}$$

The radiation conductance for short slots, $w/\lambda_o \ll 1$, is proportional to the square of length. The directivity of a short slot therefore approaches a constant value 3 which is equivalent to 4.8 dB. The radiation conductance for a long slot is proportional to the length of the slot and Eq. (16) simplifies to:

$$D_o = 4 \cdot \frac{w}{\lambda_o} \qquad \frac{w}{\lambda_o} \gg 1 \quad . \tag{17}$$

The directivity of an isolated slot is plotted in Figure 13 as a function of the length. Subject to the restrictions on h mentioned earlier, the directivity is independent of the ground plane spacing.

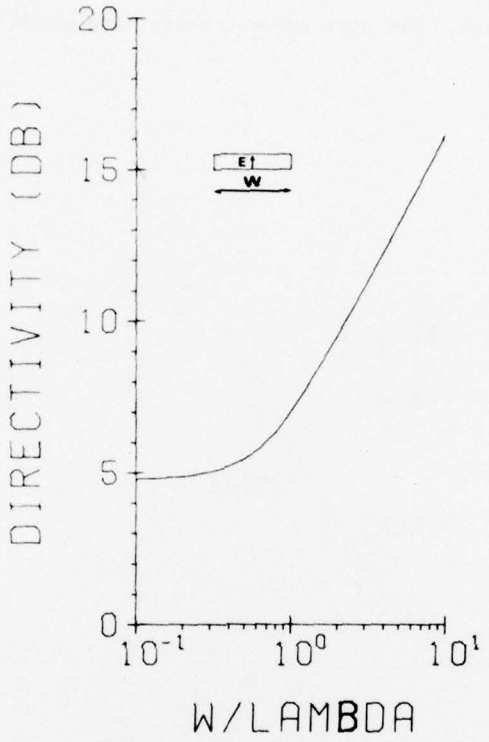

Figure 13. Directivity of a Narrow Slot With Uniform Field Distribution

7.2 Patches

The microstrip element is considered as an array of two slots spaced a distance L along the E-plane. The directivity of a patch can thus be expressed as the directivity of a slot times the contribution due to the array factor. For odd mode excitations, the latter contribution at broadside is:

$$D_{AF} = \frac{2}{1 + g_{12}} \tag{18}$$

where g_{12} is the normalized mutual conductance, as shown in Figure 9, between two slots along the E-plane.

The relative directivity of a patch is plotted in Figure 14 as a function of the length. As the length of the element increases, the directivity increases until a grating lobe appears in visible space which is the case for higher order mode resonances. A relative directivity of 3 dB is achieved when the mutual coupling between the slots is zero. The even modes always have a null in the radiation pattern at broadside.

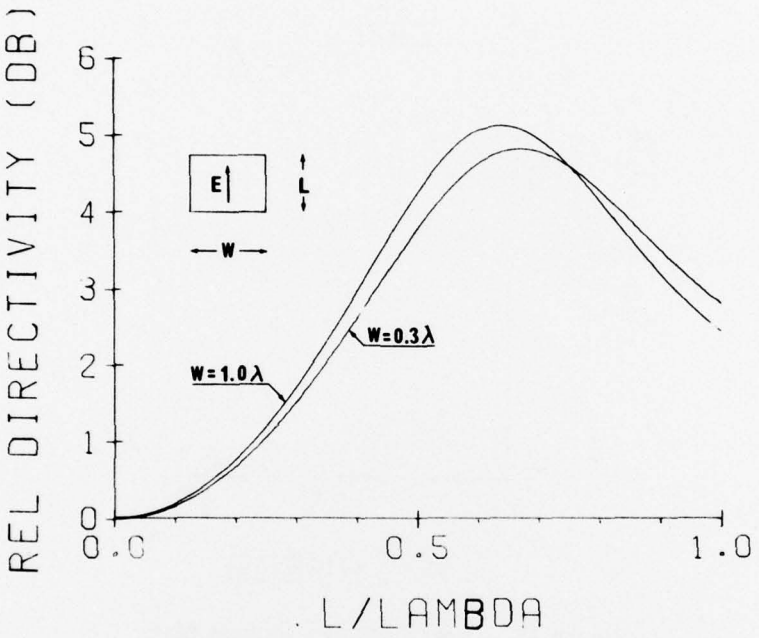

Figure 14. Relative Directivity of a Rectangular Microstrip Element at Resonance

8. CONCLUSION

The rectangular microstrip element is treated as a line resonator. The radiation takes place predominantly from the fringing fields at the open-circuited ends. This has been verified by liquid crystal displays. These fields also represent an extension of the element, making the physical resonant length just shorter than a multiple of a half dielectric wavelength.

Calculations of the input impedance show that by varying the feed point along the transmission line, the element can be matched to all practical impedance levels. From a radiation point of view, the element is considered as a pair of slots. The mutual effect between the radiating ends generally decreases the input impedance.

The mutual coupling between elements can be seen as composed of coupling between the ends of one element and both ends of the other element. Calculations show that, as expected, the mutual effect is stronger along the E-plane than along the H-plane.

References

1. Howell, J.Q. (1975) Microstrip antennas, IEEE Trans. Antennas Propagat. AP-23:90-93.
2. Munson, R.E. (1974) Conformal microstrip antennas and microstrip phased arrays, IEEE Trans. Antennas Propagat. AP-22:74-78.
3. Derneryd, A.G. (1976) Linearly polarized microstrip antennas, IEEE Trans. Antennas Propagat. AP-24:846-851.
4. Agrawal, P.K. and Bailey, M.C. (1976) An analysis technique for microstrip antennas, IEEE Society on Antennas Propagat. Int. Symp. :395-398.
5. Kaloi, C.M. (1975) Asymmetrically Fed Electric Microstrip Dipole Antenna, Report TP-75-03, Naval Missile Center, Point Magu, CA.
6. Black, L.M., and McCorkle, J.W. (1975) A Preliminary Report on the In-house Exploratory Development Program on Microstrip Patch Antennas at Naval Surface Weapons Center, Report NSWC/WOL/TR 75-200, Naval Surface Weapons Center, Silver Spring, MD.
7. Kernweis, N.P., and McIlvenna, J.F. Liquid crystal diagnostic techniques aid microstrip antenna design, pending publication in Microwave Journal.

METRIC SYSTEM

BASE UNITS:

Quantity	Unit	SI Symbol	Formula
length	metre	m	...
mass	kilogram	kg	...
time	second	s	...
electric current	ampere	A	...
thermodynamic temperature	kelvin	K	...
amount of substance	mole	mol	...
luminous intensity	candela	cd	...

SUPPLEMENTARY UNITS:

plane angle	radian	rad	...
solid angle	steradian	sr	...

DERIVED UNITS:

Acceleration	metre per second squared	...	m/s
activity (of a radioactive source)	disintegration per second	...	(disintegration)/s
angular acceleration	radian per second squared	...	rad/s
angular velocity	radian per second	...	rad/s
area	square metre	...	m
density	kilogram per cubic metre	...	kg/m
electric capacitance	farad	F	A·s/V
electrical conductance	siemens	S	A/V
electric field strength	volt per metre	...	V/m
electric inductance	henry	H	V·s/A
electric potential difference	volt	V	W/A
electric resistance	ohm		V/A
electromotive force	volt	V	W/A
energy	joule	J	N·m
entropy	joule per kelvin	...	J/K
force	newton	N	kg·m/s
frequency	hertz	Hz	(cycle)/s
illuminance	lux	lx	lm/m
luminance	candela per square metre	...	cd/m
luminous flux	lumen	lm	cd·sr
magnetic field strength	ampere per metre	...	A/m
magnetic flux	weber	Wb	V·s
magnetic flux density	tesla	T	Wb/m
magnetomotive force	ampere	A	...
power	watt	W	J/s
pressure	pascal	Pa	N/m
quantity of electricity	coulomb	C	A·s
quantity of heat	joule	J	N·m
radiant intensity	watt per steradian	...	W/sr
specific heat	joule per kilogram-kelvin	...	J/kg·K
stress	pascal	Pa	N/m
thermal conductivity	watt per metre-kelvin	...	W/m·K
velocity	metre per second	...	m/s
viscosity, dynamic	pascal-second	...	Pa·s
viscosity, kinematic	square metre per second	...	m/s
voltage	volt	V	W/A
volume	cubic metre	...	m
wavenumber	reciprocal metre	...	(wave)/m
work	joule	J	N·m

SI PREFIXES:

Multiplication Factors	Prefix	SI Symbol
1 000 000 000 000 = 10^{12}	tera	T
1 000 000 000 = 10^{9}	giga	G
1 000 000 = 10^{6}	mega	M
1 000 = 10^{3}	kilo	k
100 = 10^{2}	hecto*	h
10 = 10^{1}	deka*	da
0.1 = 10^{-1}	deci*	d
0.01 = 10^{-2}	centi*	c
0.001 = 10^{-3}	milli	m
0.000 001 = 10^{-6}	micro	μ
0.000 000 001 = 10^{-9}	nano	n
0.000 000 000 001 = 10^{-12}	pico	p
0.000 000 000 000 001 = 10^{-15}	femto	f
0.000 000 000 000 000 001 = 10^{-18}	atto	a

* To be avoided where possible

MISSION
of
Rome Air Development Center

RADC plans and conducts research, exploratory and advanced development programs in command, control, and communications (C^3) activities, and in the C^3 areas of information sciences and intelligence. The principal technical mission areas are communications, electromagnetic guidance and control, surveillance of ground and aerospace objects, intelligence data collection and handling, information system technology, ionospheric propagation, solid state sciences, microwave physics and electronic reliability, maintainability and compatibility.

Printed by
United States Air Force
Hanscom AFB, Mass. 01731